DALTON
FULL PAPER

Synthesis of π-conjugated cobaltadithiolene cyclotrimers and significant effects of electrolyte cation and solvent on their electrochemical, optical and magnetic properties †

Hiroshi Nishihara,*[a] Mika Okuno,[b] Noriko Akimoto,[b] Naho Kogawa[b] and Kunitsugu Aramaki[b]

[a] *Department of Chemistry, School of Science, The University of Tokyo, Hongo, Bunkyo-ku, Tokyo 113-0033, Japan*
[b] *Department of Chemistry, Faculty of Science and Technology, Keio University, Hiyoshi, Kohoku-ku, Yokohama 223, Japan*

A new class of cobalt cyclic trinuclear complexes with four fused aromatic rings, $[Co_3(\eta\text{-}C_5H_5)_3(S_6C_6)]$ and $[Co_3(\eta\text{-}C_5H_4Me)_3(S_6C_6)]$, was synthesized by a condensation reaction of $[Co(\eta\text{-}C_5H_5)(S_2C_2H_2)]$ and $[Co(\eta\text{-}C_5H_4Me)(S_2C_2H_2)]$, respectively, in aqueous halogenoacid solution. The complexes undergo reversible three-step $1e^-$ reductions in aprotic media forming two mixed-valence states, with overall charges 1− and 2−. The thermodynamic stability of the mixed-valence complexes estimated from the redox potential differences and the degree of internuclear electronic interaction evaluated from the intervalence-transfer bands depends markedly on the size of the electrolyte cation and the solvent polarity; larger cations and more polar solvents increase the stability and the electronic interaction. The EPR spectra of $[Co_3(\eta\text{-}C_5H_5)_3(S_6C_6)]$ reduced by $[Co(\eta\text{-}C_5Me_5)_2]$ in propylene carbonate (pc) indicate that the 1− and 3− species are paramagnetic with $S = \frac{1}{2}$, whereas the 3− species formed by reduction with Na in thf gives a spectrum of the quartet state ($S = \frac{3}{2}$) denoting ferromagnetic interaction. This difference is attributed to a weaker internuclear interaction caused by a stronger electrostatic effect of the smaller counter ion, Na^+ in thf, compared to $[Co(\eta\text{-}C_5Me_5)_2]^+$ in pc.

Metalladithiolene complexes are a family of intriguing molecules exhibiting reversible redox activity, deep color and various chemical reactivity.[1] As for (η^5-cyclopentadienyl)-(ethylene-1,2-dithiolato)cobalt, $[Co(\eta\text{-}C_5H_5)(S_2C_2H_2)]$ initially reported by King and Eggers,[2] a variety of its substituted compounds have been synthesized and their properties and reactions extensively investigated.[1,3,4]

On the other hand, internuclear electronic interactions in transition metal multinuclear complexes are of recent growing interest.[5] Several types of cyclic trinuclear complexes have been reported, most of which are oxygen or sulfur atom-bridged[6] and examples with aromatic backbones are few.[7,8] In this study we developed a new class of trinuclear complexes made of three metalladithiolene rings bound to a benzene ring, that we call 'windmill complexes'. Three cobalt sites in the complexes are electronically communicated through π-conjugated linkers so as to form two mixed valence states as manifested in the electrochemical and optical properties, of which preliminary results have been presented.[9] We report here the details of the synthesis and physical properties of these complexes. We have found significant matrix effects on their electrochemical, optical and magnetic properties.

Experimental

Monomer complexes, $[Co(\eta\text{-}C_5H_5)(S_2C_2H_2)]$ **1a** and $[Co(\eta\text{-}C_5H_4Me)(S_2C_2H_2)]$ **1b** were prepared according to the methods of King and Eggers;[2] $[Co(\eta\text{-}C_5Me_5)_2]$ was prepared as described in the literature[10] and purified by vacuum sublimation before use. Anhydrous solvents except for propylene carbonate (pc) and dmso were obtained from Kanto Chemicals. Tetra-*n*-butylammonium perchlorate and anhydrous pc were supplied by Tomiyama Chemicals as lithium battery grade. Anhydrous dmso was from Aldrich. Dichloromethane used for electrochemical measurements was an HPLC grade chemical from Kanto Chemicals. The IR, UV/VIS/NIR and EPR spectra were recorded with Shimadzu FT-IR 8100M, JASCO V-570 and JEOL JES-E300/RE3X spectrometers, respectively, ^1H and ^{13}C NMR spectra with a JEOL GX400 spectrometer. Measurements of field desorption (FD) mass spectra were carried out at UBE Scientific Analytical Laboratory.

Syntheses

Complexes 2a and 3a. Oligomerization of complex **1a** was carried out under several conditions. A typical procedure to synthesize **2a** and **3a** is as follows.

To a 150 dm^3 acetonitrile solution of complex **1a** (270 mg, 1.3 mmol) was added slowly 48% HBr (50 dm^3, 0.44 mol) with stirring and the mixture was further stirred for 17.5 h at room temperature. The solution was transferred to a separatory funnel, and Na_2CO_3 (24 g) and the minimum volume of water to dissolve the salt were added in order to neutralize the solution. After chloroform was added and the components soluble in chloroform were extracted several times, the organic layer was collected and dried with anhydrous Na_2SO_4. The solution was condensed under reduced pressure and chromatographed on a silica gel column with chloroform as an eluent. The first three bands were collected together and the fourth blue band containing the cyclic trimer **3a** was separated. The solution containing the first three bands was evaporated and chromatographed again on a silica gel column with chloroform–hexane (8:3). The second bluish green band containing the dimer **2a** was collected. The oligomers **2a** and **3a** were recrystallized thrice from chloroform–hexane and their yields were 4.3 (1.6) and 7.2 mg (2.6%), respectively. Complex **2a** (Found: C, 39.29; H, 3.06. $C_7H_6CoS_2$ requires C, 39.44; H, 2.84%): *m/z* (FD) 426, M^+; ^1H NMR ($CDCl_3$) δ 9.28 (2 H, s, CH) and 5.34 (10 H, s, C_5H_5); FTIR (KBr, $\tilde{\nu}/cm^{-1}$) 3090, 1410, 1397, 1341,

† *Supplementary data available*: plots of yields *vs.* time, log K_c *vs.* Stokes' radius and LUMOs. For direct electronic access see http://www.rsc.org/suppdata/dt/1998/2651/, otherwise available from BLDSC (No. SUP 57404, 6 pp.) or the RSC Library. See Instructions for Authors, 1998, Issue 1 (http://www.rsc.org/dalton).

1188, 1105, 1094, 999, 895, 849, 776 and 762; λ_{max}/nm (ε/dm^3 mol^{-1} cm^{-1}) 780 (4800), 640 (18 300), 352 (13 000), 300 (44 000) and 236 (23 000). Complex **3a** (Found: C, 39.28; H, 2.53; S, 29.98. $C_7H_5CoS_2$ requires C, 39.62; H, 2.38; S, 30.23%): *m*/*z* (FD) 636, M^+; ^{1}H NMR ($CDCl_3$) δ 5.45 (15 H, s, C_5H_5); ^{13}C-{^{1}H} NMR ($CDCl_3$) δ 79.56 (C_5H_5); FTIR (KBr, $\tilde{\nu}$/cm^{-1}) 3090, 1412, 1341, 1100, 1051, 1001 and 830; λ_{max}/nm (ε/dm^3 mol^{-1} cm^{-1}) 688 (30 000), 360 (7200), 308 (98 000) and 234 (30 000).

Complexes 2b and 3b. A reaction of complex **1b** (50.0 mg, 0.219 mmol) and 48% HBr (8.64 dm^3, 76.0 mmol) in MeCN (25.4 dm^3) was carried out in a similar manner to that described for **1a** at room temperature for 2 h. Components in the product were separated by silica gel column chromatography using chloroform–hexane (4:1) as an eluent. The dimer **2b** was purified using a JAI LC-908 recycling HPLC apparatus with JAIGEL-2H and -3H columns. The cyclic trimer **3b** was thoroughly rinsed with toluene and recrystallized from CH_2Cl_2–hexane. Yields of **2b** and **3b** were 4.2 and 1.5%, respectively. Complex **2b** (Found: C, 42.87; H, 4.16. $C_8H_8CoS_2$ requires C, 42.59; H, 3.89%): ^{1}H NMR ($CDCl_3$) δ 9.19 (2 H, s, CH), 5.22 (2 H, t, J = 1.98 Hz, C_5H_5), 5.09 (2 H, t, C_5H_5) and 2.24 (s, 6 H, Me); FTIR (KBr, $\tilde{\nu}$/cm^{-1}) 3090, 3071, 2921, 2853, 1561, 1509, 1474, 1458, 1422, 1383, 1364, 1264, 1022, 918 and 833; λ_{max}/nm (ε/dm^3 mol^{-1} cm^{-1}) 790 (sh), 647 (14 000), 302 (35 800) and 237 (20 500). Complex **3b** (Found: C, 42.48; H, 3.12. $C_8H_7CoS_2$ requires C, 42.22; H, 3.24%): *m*/*z* 678 (FD), M^+; ^{1}H NMR ($CDCl_3$) δ 5.33 (6 H, t, J = 1.98 Hz) and 5.29 (6 H, s); FTIR (KBr, $\tilde{\nu}$/cm^{-1}) 3081, 3067, 2921, 2853, 1561, 1509, 1474, 1458, 1422, 1383, 1364, 1264, 1022, 918, 833 and 419; λ_{max}/nm (ε/dm^3 mol^{-1} cm^{-1}) 696 (23 300), 311 (78 200) and 230 (24 200).

The dependence of the yields of complexes **2a**, **3a**, **2b** and **3b** on the reaction conditions was studied based on GPC chromatograms recorded with a JAI LC-908 recycling preparative HPLC apparatus with JAIGEL-2H and -3H columns.

Electrochemical measurements

A glassy-carbon rod (outside diameter 5.0 mm, Tokai Carbon GC-20) was embedded in Pyrex glass and the cross-section used as a working electrode. Its surface was polished with 0.3 μm alumina abrasive, sonicated in distilled water and in acetone, dried, and used for electrochemical measurements. Cyclic voltammetry and differential-pulse voltammetry were carried out in a standard three-compartment cell under an argon atmosphere at 25 °C equipped with a platinum wire counter electrode and an Ag–Ag$^+$ reference electrode [10 mmol dm^{-3} $AgClO_4$ in 0.1 mol dm^{-3} NBu_4ClO_4–MeCN, $E^{\circ\prime}$ (ferrocenium–ferrocene) = 0.20 V *vs.* Ag–Ag$^+$] with a BAS CV-50W voltammetric analyzer.

Electronic spectra of the reduced forms of complexes 3a and 3b

Reduced forms of complexes **3a** and **3b** were prepared by three methods; electrochemical reduction, chemical reduction with Na in thf and that with [Co(η-C_5Me_5)$_2$] in pc. Then their UV/VIS/NIR spectra were measured. Electrochemical reduction was carried out at a given potential to form mono-, di- or trivalent anions in a three-compartment cell with coulometry in an argon-filled dry box, then the fully electrolyzed solution was transferred to a sealed quartz cell for the measurement.

A Pyrex glass tube with a branch room for preparing sodium mirror and a 10 × 10 mm quartz spectrometric cell was used for the chemical reduction with Na. After a sample and Na were placed in the glass tube and the branch room, respectively, the cell was connected to a high vacuum line and evacuated, then a sodium mirror was deposited and thf was transferred to the tube by vacuum distillation. Finally, the glass tube was sealed off under vacuum. Stepwise reduction of the sample was carried out by contacting the solution with the sodium mirror.

A quartz cell connected to a Pyrex glass tube with six small branch rooms to keep the reducing agent was used for the [Co(η-C_5Me_5)$_2$]–pc system. In a dry-box, a given volume of a hexane solution of [Co(η-C_5Me_5)$_2$] was put in each branch and the solvent was carefully evaporated to yield solid [Co(η-C_5Me_5)$_2$] in the branches. Then a pc solution of complex **3a** was introduced in the cell and the cell closed with a stopcock. Outside the dry-box, spectra of the reduced forms were measured after the sample solution was mixed in step with the reducing agent in six branches. This manipulation was repeated to get a series of spectral changes in the reduction process.

Table 1 Reaction conditions[a] and yields of complexes **2a** and **3a** from **1a**

		Yield (%)		
Solvent	Acid	**2a**	**3a**	**1a** (recovered)
CH_2Cl_2–EtOH (1:3)	Conc. HCl	0.4	0.2	>32
thf	Conc. HCl	3.2	0.5	>29
acetone	Conc. HCl	*b*	*b*	>29
MeCN	Conc. HCl	4.2	3.6	31.1
MeCN	48% HBr	6.5	3.2	10.4
MeCN[c]	48% HBr	2.7	1.2	3.3
MeCN[d]	48% HBr	0.8	0.5	13.1
MeCN	55% HI	*b*	*b*	*b*
MeCN	Conc. H_2SO_4	*b*	*b*	>31
MeCN	Conc. HNO_3	*b*	*b*	*b*
MeCN	$MeCO_2H$	*b*	*b*	>29

[a] Room temperature in air for 17 h unless otherwise stated. [b] Less than 0.1%. [c] Under O_2. [d] Under N_2.

EPR spectroscopy

The EPR spectra were measured for complexes **3a** and **3b** and their three reduced forms. A 5 mm diameter EPR tube was connected to the cell used for the UV/VIS/NIR measurement of the Na–thf system as noted above. After the reduction of **3a** and **3b** with Na had been monitored by the electronic spectra, a part of the sample solution was transferred to the EPR tube, sealed off under vacuum and its EPR spectrum measured. The sample reduced by [Co(η-C_5Me_5)$_2$]–pc was prepared in a dry-box by adding a given amount of a hexane solution of [Co(η-C_5Me_5)$_2$] to a pc solution of **3a**. The solution was transferred to an EPR tube connected with a three-way vacuum cock and degassed in vacuum thrice, then sealed in vacuum.

Molecular orbital calculations

The molecular structure of complex **3a** was optimized using the ZINDO/1 method with the default parameters on the computer program, HYPERCHEM (Hypercube Inc.).[11] Assuming that **3a** belongs to the point group C_{3v}, its geometry was taken from the averaged values. The assumed bond distances in Å were as follows: Co–S 2.258, Co–C 2.130, C–H 1.091, C–C 1.394 and C–S 1.780. Molecular orbital calculations were carried out using the ZINDO/S method with the same program using default parameters.

Results and Discussion

Synthesis and characterization of the windmill complexes

Oligomerization of the monomer **1a** occurs in acidic media in air, affording a dimer **2a**, cyclic trimer **3a** and insoluble precipitates which may contain polymeric components. Table 1 gives yields of **2a** and **3a** under several conditions. When HCl is used as acid the yield of **3a** is higher when the solvent is in the order CH_2Cl_2 < thf < MeCN. Halogenoacids, HCl and HBr, are better for the synthesis of both **2a** and **3a** than other acids.

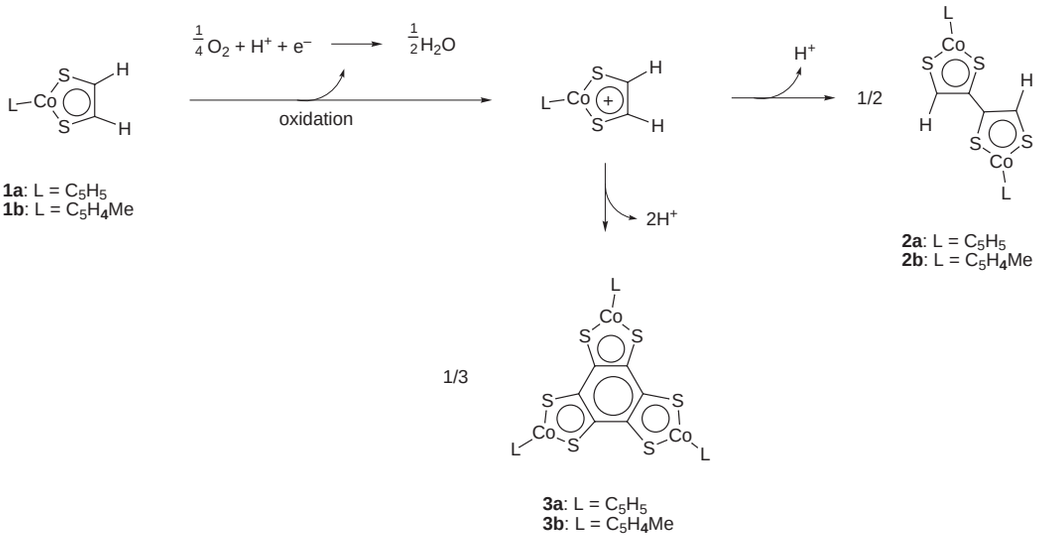

Scheme 1

A similar coupling reaction of a cobaltadithiolene complex has recently been reported in a Friedel–Crafts acetylation conditions by Kajitani *et al.*[4]

Investigation of the time-course changes in the yields of complexes **2a** and **3a** in the reaction with HBr in MeCN (see SUP 57404) has revealed that the yields increase during the first 18 h reaching a maximum, then decrease gradually, indicating coexistence of formation and decomposition reactions. The best yield of **3a** was 6.5%. The decrease should be due to a higher oligomerization reaction and/or oxidative decomposition of the cobaltadithiolene structure as judged from the electrochemical properties (see below). Yields of the oligomers are much lower in the reaction under nitrogen, indicating that O_2 is involved. However, the reaction under oxygen for 17 h gives lower yields than that in air. This is probably due to the further progress of the oligomerization and/or oxidative decomposition of the cobaltadithiolene structure since the amount of recovered monomer is low. Based on these results, we deduce the mechanism as shown in Scheme 1, where the oxidation by O_2 and H^+ yields a cation radical followed by coupling and deprotonation affording the dimer and trimer. It should be noted that we could not detect the linear trimer, $H[(C_2S_2)Co(\eta\text{-}C_5H_5)]_3H$. This might be due to its thermodynamic instability because the steric repulsion between S atoms in the neighboring dithiolatocobalt rings prevents the formation of a coplanar structure.

Similar dimerization and cyclotrimerization reactions occur when the monomer is a methylcyclopentadienyl complex, **1b**. The coupling reactions of **1b** with HBr in MeCN at room temperature forming **2b** and **3b** are faster compared to that of **1a**, which is attributed to the more facile oxidation of **1b** compound to that of **1a** due to the electron-donating effect of the methyl group. The maximum yield of **3b** was 4% at the reaction time of 3 h. It should be noted that our trials to prepare oligomer complexes by the reaction of $[Co(\eta^5\text{-}MeOCOC_5H_4)(S_2C_2H_2)]$ and $[Co(\eta\text{-}C_5Me_5)(S_2C_2H_2)]$ in various acidic solutions have failed.

Dinuclear complexes, **2a** and **2b**, and trinuclear complexes, **3a** and **3b**, were characterized by elemental analysis, FD-MS, ^1H, ^{13}C NMR, IR and UV/VIS spectra. The ^1H NMR spectra of **3a** and **3b** show no signals at δ 8–9 in the region for protons on cobaltadithiolene rings. Signals ascribed to three C_5H_5 and C_5H_4Me rings in **3a** and **3b**, respectively, are not distinguished, indicating their structural equivalence. These results and mass spectral data confirm the cyclic trinuclear structure of **3a** and **3b**. In a $^{13}C\text{-}\{^1H\}$ NMR spectrum of **3a** we could detect only a peak due to carbons of the C_5H_5 rings at δ 79.56 due to the low solubility of **3a** in $CDCl_3$ and the carbons on the benzene ring

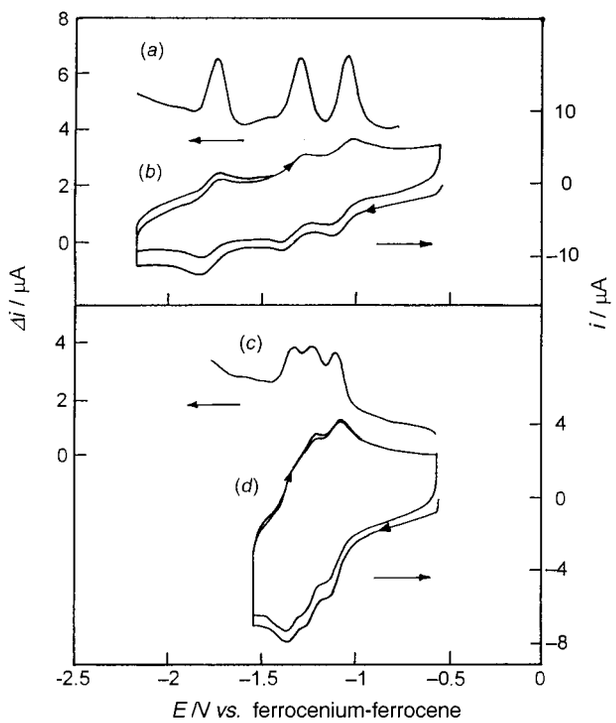

Fig. 1 Differential-pulse voltammograms at 0.02 V s^{-1} (*a*, *c*) and cyclic voltammograms at 0.1 V s^{-1} (*b*, *d*) of complex **3a** at glassy carbon in 0.1 mol dm^{-3} NBu_4ClO_4–thf (*a*, *b*) and in $NaBPh_4$–thf (*c*, *d*)

have no NOE. In the UV/VIS spectra of **3a** and **3b** a strong absorption peak with $\varepsilon = (2\text{–}3) \times 10^4$ dm^3 mol^{-1} cm^{-1} is seen at *ca.* 700 nm, which is attributed to the LMCT band from S to Co as usually seen for metalladithiolene complexes.[12] This band appears at 551, 640, 588 and 647 nm for **1a**, **2a**, **1b** and **2b**, respectively. The red shift of the band with the increase in the number of nuclei from **1** to **2** and **3** can be ascribed to the effect of expansion in conjugation length.

Electrochemical properties

Electrochemical measurements on complex **3a** were carried out in various electrolyte solutions and two examples of the results, differential-pulse voltammograms and cyclic voltammograms in NBu_4ClO_4–thf and in $NaBPh_4$–thf, are displayed in Fig. 1. Three $1e^-$ reduction waves appear for every solution, while the baseline effects are large due to low solubility of **3a** in any solvent. The appearance of three waves indicates formation of

Table 2 Redox properties of complexes **3a** and **3b**

Complex	Electrolyte[a]	$E^{\circ\prime}$ for reduction *vs.* ferrocenium–ferrocene 1st	2nd	3rd	$\Delta E^{\circ\prime}_{12}$/V	$\Delta E^{\circ\prime}_{23}$/V	log K_{c1}	log K_{c2}
3a	NBu_4ClO_4–thf	−1.06	−1.30	−1.74	0.24	0.44	4.1	7.4
	NBu_4BPh_4–thf	−0.88[b]	−1.44[b]	−1.56[b]	0.27	0.41	4.6	6.9
	$LiClO_4$–thf	−1.18	−1.39	−1.57	0.21	0.18	3.6	3.0
	$LiClO_4$–thf[c]	−1.01	−1.22	−1.61	0.21	0.39	3.6	6.9
	$NaBPh_4$–thf	−1.11	−1.25	−1.36	0.14	0.11	2.4	1.9
	$NaBPh_4$–thf[d]	−1.06	−1.32	−1.67	0.26	0.35	4.4	5.9
	$NaBPh_4$–thf[e]	−1.11	−1.43	−1.80	0.32	0.37	5.4	6.3
	$NaClO_4$–thf[f]	−1.14	−1.28	−1.40	0.14	0.12	2.4	2.1
	NBu_4ClO_4–MeCN	−0.96	−1.22	−1.61	0.26	0.39	4.4	6.6
	NBu_4BPh_4–MeCN	−0.90[b]	−1.15[b]	−1.54[b]	0.25	0.39	4.2	6.9
	NEt_4ClO_4–MeCN	−1.01	−1.21	−1.54	0.20	0.33	3.4	5.6
	NMe_4BF_4–MeCN[g]	−1.00	−1.21	−1.50	0.21	0.29	3.5	4.9
	$LiClO_4$–MeCN	−0.96	−1.20	−1.44	0.24	0.24	4.1	4.1
	$NaBPh_4$–MeCN	−0.96	−1.19	−1.33	0.23	0.20	3.9	3.4
	NBu_4ClO_4–dmf	−0.99	−1.27	−1.68	0.28	0.41	4.7	6.9
	NMe_4BF_4–dmf[d]	−1.00	−1.27	−1.60	0.27	0.33	4.6	5.6
	$LiClO_4$–dmf	−1.00	−1.31	−1.73	0.31	0.42	5.2	7.1
	$NaBPh_4$–dmf	−1.00	−1.29	−1.63	0.29	0.34	4.9	5.7
	NBu_4ClO_4–dmso	−0.95	−1.22	−1.60	0.27	0.38	4.6	6.4
	NMe_4BF_4–dmso[d]	−0.95	−1.21	−1.56	0.26	0.35	4.4	5.9
	$LiClO_4$–dmso	−0.94	−1.21	−1.60	0.27	0.38	4.6	6.6
	$NaBPh_4$–dmso	−0.95	−1.22	−1.60	0.27	0.39	4.6	6.4
3b	NBu_4ClO_4–thf	−1.13	−1.36	−1.80	0.23	0.44	3.9	7.4
	$NaBPh_4$–thf	−1.16	−1.27	−1.39	0.11	0.12	1.9	2.1
	$NaBPh_4$–thf[e]	−1.16	−1.38	−1.50	0.22	0.12	3.7	2.1
	NBu_4ClO_4–MeCN	−1.03	−1.29	−1.66	0.26	0.37	4.4	6.3

[a] Concentration was 0.1 mol dm^{-3} unless otherwise stated. [b] *vs.* $Ag–Ag^+$. [c] Added 0.25 mol dm^{-3} 12-crown-4. [d] Added 0.2 mol dm^{-3} 15-crown-5. [e] Added 0.2 mol dm^{-3} 18-crown-6. [f] Saturated (<0.4 mol dm^{-3}). [g] Saturated (<0.1 mol dm^{-3}).

two mixed valence states, $Co^{II}Co^{III}Co^{III}$ and $Co^{II}Co^{II}Co^{III}$, in the intermediate reduction stages, although the redox potential depends on the type of solvent and electrolyte. The number of electrons consumed at each step was confirmed to be one by coulometry. Table 2 summarizes the results in various electrolyte solutions of alkali metal salts and tetraalkylammonium salts for **3a** and **3b**.

Conproportionation constants,[13] K_{c1} and K_{c2}, in equations (1) and (2) were calculated from the redox potential differences

$$K_{c1} = [\mathbf{3}^-]^2/[\mathbf{3}][\mathbf{3}^{2-}] = \exp(|E_1^{\circ\prime} - E_2^{\circ\prime}|F/RT) \quad (1)$$

$$K_{c2} = [\mathbf{3}^{2-}]^2/[\mathbf{3}^-][\mathbf{3}^{3-}] = \exp(|E_2^{\circ\prime} - E_3^{\circ\prime}|F/RT) \quad (2)$$

between $\mathbf{3}^{0/1-}$ and $\mathbf{3}^{1-/2-}$ and between $\mathbf{3}^{1-/2-}$ and $\mathbf{3}^{2-/3-}$ according to equations (1) and (2), respectively, are given in Table 2. The general tendency is that the redox potentials depend on the cation size; the larger the size, the higher are the K_{c1} and K_{c2} values as is seen in a series of tetraalkylammonium ions in MeCN. Alkali metal ions give smaller K_c values compared to tetraalkylammonium ion. It should be noted that K_{c1} is larger than K_{c2} in MeCN with alkali metal ion, but the opposite in other solutions. Addition of crown ethers to the solution of alkali metal ions increases K_c values as is noted in Table 2. Simulation of the dependence on the concentration of crown ether using the complexation constants of crown ether with the cation obtained by conductivity analysis and several equations concerning association, ion-pairing equilibrium, conproportionation and charge balance, assuming that most of $\mathbf{3a}^-$, $\mathbf{3a}^{2-}$ and $\mathbf{3a}^{3-}$ exists in the form of ion pairs, has been reported in a separate paper.[14]

Table 2 also indicates a strong dependence on solvent; a solvent with higher polarity tends to give higher K_c values. Dependence of K_c on both the cation size and the solvent polarity indicates that the solvated cation size dominates the K_c values. Plots of log K_c for complex **3a** *vs.* the Stokes' radius, r_s, (see SUP 57404) show a positive dependence for all the combinations of solvent and electrolyte salt, although the slopes and magnitudes are different for the different types of solvent and cation. It can be expected that the cation as the counter ion of anionic forms of **3** can be either non-solvated, weakly solvated or strongly solvated, which might be a rationale for why K_c does not correlate to r_s simply.

Cyclic voltammetry for the oxidation reaction of complexes **1a**, **2a** and **3a** in 0.1 mol dm^{-3} NBu_4ClO_4–MeCN at 0.1 V s^{-1} at room temperature shows an irreversible oxidation peak at 0.38, 0.08 and −0.08 V *vs.* ferrocenium–ferrocene, respectively. This indicates that the oxidative decomposition of **3a**, which occurs more easily than **1a** and **2a**, can be a cause of the yield decrease in the reaction at longer times or under O_2 as mentioned above.

Intervalence-transfer bands

Three reduced forms of complexes **3a** and **3b** were generated by both electrochemical and chemical methods and their UV/VIS/NIR spectra observed. Fig. 2 presents the spectra for four oxidation states of **3a** when it is reduced chemically by Na in thf and by $[Co(\eta\text{-}C_5Me_5)_2]$ in pc. The spectra in the UV/VIS region are similar to each other in all reducing media except for overlapping with the spectrum of $[Co(\eta\text{-}C_5Me_5)_2]^+$ in Fig. 2(*b*)–2(*d*) at wavelengths below 500 nm. The LMCT band at 700 nm decreases according to the progress of the reduction and finally disappears on reaching the trivalent anion. The absorption below 500 nm increases with the reduction, and consequently, the solution changes from blue, bluish green, green to light orange corresponding to the neutral form and mono-, di- and tri-valent anions.

Matrix effects on the intervalence transfer (IT) band of mixed-valence complexes have been reported for several systems such as $[(NH_3)_5Ru^{III}(pyz)Ru^{II}Cl(2,2'\text{-bpy})_2]^{4+}$,[15] $[(NH_3)_5Ru^{III}(4,4'\text{-bpy})Ru^{II}(NH_3)_5]^{5+}$[16] or $[(NH_3)_5RuLRu(2,2'\text{-bpy})_2LRu(NH_3)_5]$ [L = pyrazine (pyz), 4,4′-bpy, *trans*-1,2-bis(4-pyridyl)ethylene or 1,2-bis(4-pyridyl)ethane].[17] The mixed-valence states of **3a** give IT bands in the NIR region as shown

in Fig. 2, where the intensity for $\mathbf{3a}^{2-}$ formed by chemical reduction depends markedly on the type of solvent and counter ion. A similar dependence was also observed in the spectra of the electroreduced forms of **3a** in different electrolyte solutions. Complex **3b** gives similar results.

The ν_{max}, ε_{max} and $\Delta\nu_{\frac{1}{2}}$ values were evaluated in order to compare qualitatively the matrix effects on the charge delocalization in the mixed-valence states, although the broadness of the NIR band results in less reliability in the values of weaker bands. The results are summarized in Table 3. A common method to analyze IT bands is to converge their parameters into the mixing coefficient, α, and H_{AB} representing the degree of internuclear interaction according to equations (3) and (4) of

$$\alpha^2 = (4.24 \times 10^{-4}/m_d m_a)(\varepsilon_{max}\Delta\nu_{\frac{1}{2}}\nu_{max}^{-1})r^{-2} \quad (3)$$

$$H_{AB} = \alpha\nu_{max} \quad (4)$$

Hush's theory,[18] where m_d, m_a and r are the number of donor sites, the number of acceptor sites and the donor–acceptor distance, respectively; $m_d m_a$ is 2 in both mixed-valence states of the cyclic trinuclear complex. We estimated that $r = 7.4$ Å based on the structure obtained by geometrical optimization using the ZINDO/1 method as described below, and the α values were calculated. The α and H_{AB} values for $\mathbf{3}^-$ and $\mathbf{3}^{2-}$ in various solutions are also given in Table 3. There is an apparent dependence of both values on the nature of the solvent and counter ion and a significant correlation between α and K_c values. The α value is between 0.02 and 0.04, indicating that $\mathbf{3}^-$ and $\mathbf{3}^{2-}$ can be classified as Robin and Day class II mixed-valence complexes.[19]

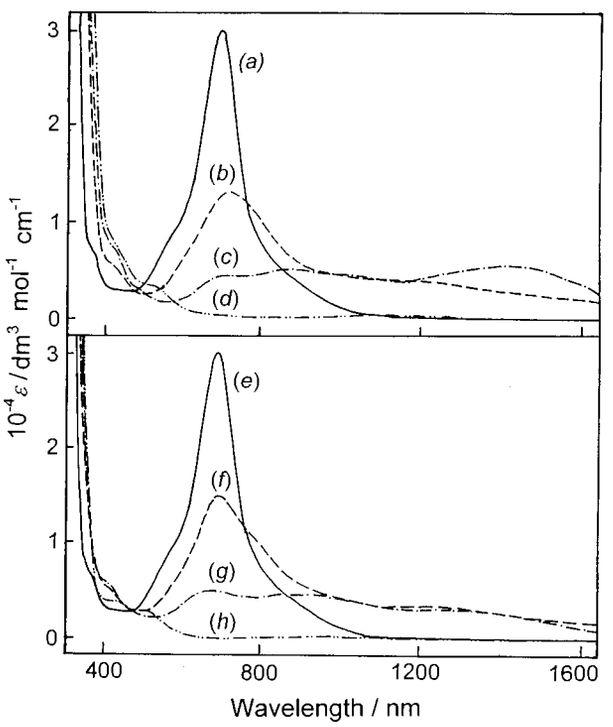

Fig. 2 The UV/VIS/NIR spectra of complex **3a** (*a*), $[Co(\eta\text{-}C_5Me_5)_2]^+\mathbf{3a}^-$ (*b*), $[Co(\eta\text{-}C_5Me_5)_2]^+{}_2\mathbf{3a}^{2-}$ (*c*) and $[Co(\eta\text{-}C_5Me_5)_2]^+{}_3\mathbf{3a}^{3-}$ (*d*) in pc, and **3a** (*e*), $Na^+\mathbf{3a}^-$ (*f*), $Na^+{}_2\mathbf{3a}^{2-}$ (*g*) and $Na^+{}_3\mathbf{3a}^{3-}$ (*h*) in thf

EPR spectra

The EPR spectra of complexes $\mathbf{3a}^-$ and $\mathbf{3a}^{3-}$ at 77 K generated by chemical reduction of **3a** with Na in thf and by $[Co(\eta\text{-}C_5Me_5)_2]$ in pc are given in Fig. 3. The $\mathbf{3a}^{2-}$ ion is EPR-silent in both media, indicating diamagnetism or antiferromagnetic interaction. The C_5H_4Me complex **3b** gives similar spectra to those of **3a** in the Na–thf system. The spectra of monoanion $\mathbf{3a}^-$ in the Na–thf and in $[Co(\eta\text{-}C_5Me_5)_2]$–pc systems are similar to each other and exhibit hyperfine splitting due to the cobalt nucleus with $I = \frac{7}{2}$. The A_z value evaluated from the splitting of the $g_\parallel$ signals for the $Na^+\mathbf{3a}^-$ in thf is 9.2 [Fig. 3(*a*)], larger than that for $[Co(\eta\text{-}C_5Me_5)_2]^+\mathbf{3a}^-$ in pc, 8.8 [Fig. 3(*b*)]. This means that the interaction of the electronic spin with the cobalt nuclear spin is stronger in the former than the latter.

The most significant feature seen in Fig. 3 is the difference in the spectra between $Na^+{}_3\mathbf{3a}^{3-}$ in thf [Fig. 3(*c*)] and $[Co(\eta\text{-}C_5Me_5)_2]^+{}_3\mathbf{3a}^{3-}$ in pc [Fig. 3(*d*)]. The latter spectrum is similar to the spectra of $\mathbf{3a}^-$ given in Fig. 3(*a*) and 3(*b*), indicating $S = \frac{1}{2}$. The A_z value is 9.1, larger than that for $[Co(\eta\text{-}C_5Me_5)_2]^+\mathbf{3a}^-$, indicating a stronger electron–cobalt nucleus interaction. On the other hand, the spectrum of $Na^+{}_3\mathbf{3}^{3-}$ in thf is the typical pattern of $S = \frac{3}{2}$ in a nearly axial field with $g = 2.057$ and $D = 0.102$ cm^{-1}.[20] This implies that the spin–spin interaction is changed drastically by the matrix effects.

Matrix effects on the charge delocalization in the windmill complex

The results for both the redox properties and IT bands of the windmill complex described above demonstrate that the charge delocalization in the mixed-valence states is considerably influenced by the counter ion and surrounding solvent. These matrix effects are related to the size of the solvated counter ion as shown in Figs. 1 and 2, where a smaller counter ion perturbs the delocalization more significantly. This can be attributed to a stronger electrostatic interaction of the complex anion with a smaller counter ion that can locate more closely to the complex ion than a larger one. The smaller A_z value for the EPR spectra

Table 3 IT Band characteristics of complexes **3a** and **3b**

Complex ion	Reduction media[a]	$\tilde{\nu}_{max}$/cm^{-1}	ε_{max}/dm^{-3} mol^{-1} cm^{-1}	$\Delta\nu_{\frac{1}{2}}$/cm^{-1}	$10^2\,\alpha$[b]	H_{AB}[b]/cm^{-1}
$\mathbf{3a}^-$	NBu_4ClO_4–thf	7810	720	1300	2.2	170
	$NaBPh_4$–thf	7840	150	900	0.8	60
	$NaBPh_4$–dmso	7970	480	1300	1.7	140
	Na–thf	8430	630	1500	2.1	180
	$[Co(\eta\text{-}C_5Me_5)_2]$–pc	8065	390	1000	1.4	120
$\mathbf{3a}^{2-}$	NBu_4ClO_4–thf	6920	3000	1500	5.0	350
	$NaBPh_4$–thf	7220	480	1800	2.1	150
	$NaBPh_4$–dmso	6970	2200	1400	4.2	290
	$[Co(\eta\text{-}C_5Me_5)_2]$–pc	6900	2200	1500	4.3	300
	Na–thf	7690	650	1600	2.3	180
$\mathbf{3b}^-$	NBu_4ClO_4–thf	7810	770	1600	2.5	190
	Na–thf	7520	240	1400	1.3	100
$\mathbf{3b}^{2-}$	NBu_4ClO_4–thf	6870	1000	1900	3.3	230
	Na–thf	7550	280	1400	1.4	110

[a] Na–thf and $[Co(\eta\text{-}C_5Me_5)_2]$–pc used for chemical reduction. Otherwise electrolyte solutions were used for electrochemical reduction. Electrolyte concentration was 0.1 mol dm^{-3} unless otherwise stated. [b] $r = 7.4$ Å is used for the calculation.

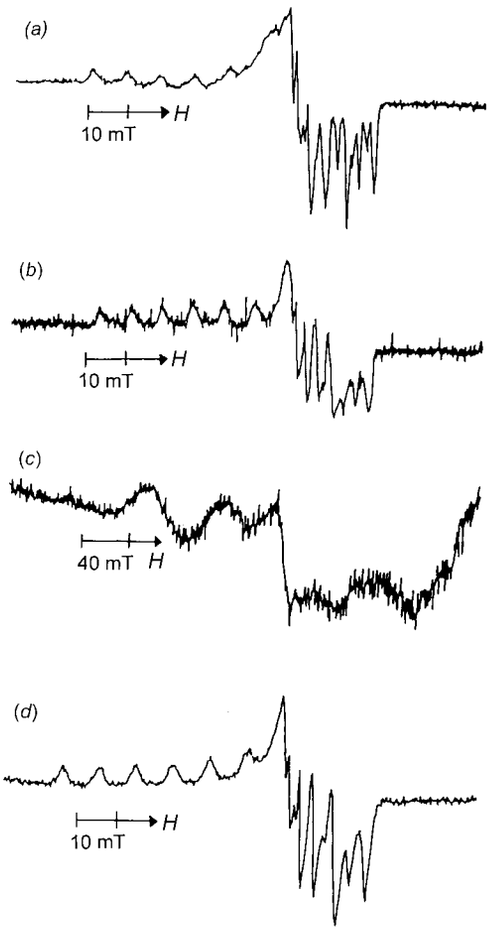

Fig. 3 The EPR spectra of 2×10^{-5} mol dm^{-3} Na^{+}**3a**$^{-}$ (*a*) and $Na^{+}{}_{3}$**3a**$^{3-}$ (*c*) in thf and 2×10^{-5} mol dm^{-3} $[Co(\eta\text{-}C_5Me_5)_2]^{+}$**3a**$^{-}$ (*b*) and $[Co(\eta\text{-}C_5Me_5)_2]^{+}{}_{3}$**3a**$^{3-}$ (*d*) in pc at 77 K. Parameters obtained are $g_{\parallel} = 2.225$, $A_z = 9.2$ and $g_{\perp} = ca.$ 2.00 for (*a*), $g_{\parallel} = 2.238$, $A_z = 8.8$ and $g_{\perp} = ca.$ 2.00 for (*b*), $g = 2.057$ and $D = 0.102$ cm^{-1} for (*c*), and $g_{\parallel} = 2.235$, $A_z = 9.1$ and $g_{\perp} = ca.$ 2.00 for (*d*)

of **3a**$^{-}$ in the $[Co(\eta\text{-}C_5Me_5)_2]$–pc system than that in the Na–thf system supports this expectation.

As the Co, 2C and 2S atoms in the cobaltadithiolene complex constitute a planar ring, **3a** can be assumed to belong to C_{3v} symmetry when three C_5H_5 rings perpendicular to the plane of 3Co, 6C and 6S atoms are fixed at the same rotation angle. As our various trials to obtain single crystals of **3a** and **3b** for X-ray crystallography have not succeeded, geometry optimization of **3a** was carried out based on this symmetry using ZINDO/1, then a molecular orbital calculation was performed using the ZINDO/S method. The LUMO thus obtained (see SUP 57404) is a_1 and doubly degenerate orbitals (e) locate slightly above it (the energy gap between these two levels is calculated to be 0.01 eV, while that between the HOMO and LUMO is 6.3 eV; 1 eV $\approx 1.60 \times 10^{-19}$ J). The a_1 and e MOs are mostly made of three cobalt $3d_{xy}$ orbitals with a slight Co–S antibonding character and their shapes are deducible from the cyclic H_3 molecule. The small energy gap between a_1 and e orbitals indicates that these MOs are mostly equivalent to the set of three localized orbitals at the cobalt sites. The latter situation should be more important when the counter ion size is smaller, because the electron(s) on the cobalt site(s) interact more strongly with the counter ion(s) so that the electrons are more localized at each cobalt site as demonstrated by the electrochemical and optical properties (see above). This is in accordance with the delicate situation that influences the magnetic properties of **3a**$^{3-}$ which changes dramatically between $S = \frac{1}{2}$ for a large counter ion $[Co(\eta\text{-}C_5Me_5)_2]^{+}$ in pc and $S = \frac{3}{2}$ for a small ion Na^{+} in thf.

Conclusion

A new class of cobaltadithiolene trinuclear complexes with four fused aromatic rings, were synthesized by deprotonative condensation reaction of $[Co(\eta\text{-}C_5H_5)(S_2C_2H_2)]$ and $[Co(\eta\text{-}C_5H_4Me)(S_2C_2H_2)]$ in aqueous acid. The internuclear electronic interaction strongly depends on the type of solvent and cation. A larger solvated cation delocalizes the negative charge more significantly, resulting in a larger separation of three redox potentials and stronger IT bands observed for the two mixed-valence states. This also leads to a change in the magnetic property of the trivalent anion, $[Co^{III}{}_{3}(\eta\text{-}C_5H_5)_3(S_6C_6)]^{3-}$, $S - \frac{1}{2}$ in the $[Co(\eta\text{-}C_5Me_5)_2]$–pc system and $S = \frac{3}{2}$ in the Na–thf system.

Acknowledgements

This work was partly supported by a Grant-in-Aid for Scientific Research from the Ministry of Education, Science, Sports and Culture, Japan 'Innovative Synthetic Reactions' No. 283 and No. 09440226) and The Asahi Glass Foundation. We thank Dr. S. Nakajima and RICOH Ltd. for the measurement of EPR spectra and Professor T. Watanabe for helpful discussion.

References

1 For some reviews, see G. N. Schrauzer, *Acc. Chem. Res.*, 1969, **2**, 72; J. A. McCleverty, *Prog. Inorg. Chem.*, 1969, **10**, 49; R. P. Burns and C. A. McAuliffe, *Adv. Inorg. Chem. Radiochem.*, 1979, **22**, 303; U. T. Mueller-Westerhoff and B. Vance, in *Comprehensive Coordination Chemistry*, eds. G. Wilkinson, R. D. Gillard and J. A. McCleverty, Pergamon, Oxford, 1987, vol. 2, pp. 595–631; A. Sugimori, *Yuki Gosei Kagaku Kyokaishi*, 1990, **48**, 788.
2 R. B. King and C. A. Eggers, *Inorg. Chem.*, 1968, **7**, 341.
3 M. Kajitani, T. Fujita, N. Hisamatsu, H. Hatano, T. Akiyama and A. Sugimori, *Coord. Chem. Rev.*, 1994, **132**, 175; M. Kajitani, T. Suetsugu, T. Takagi, T. Akiyama and A. Sugimori, *J. Organomet. Chem.*, 1995, **487**, C8; A. Sugimori, N. Tachiya, M. Kajitani and T. Akiyama, *Organometallics*, 1996, **15**, 5564; A. Sugimori, K. Yanagi, G. Hagino, M. Tamada, M. Kajitani and T. Akiyama, *Chem. Lett.*, 1997, 807.
4 M. Kajitani, G. Hagino, M. Tamada, T. Fujita, M. Sakurada, T. Akiyama and A. Sugimori, *J. Am. Chem. Soc.*, 1996, **118**, 489.
5 H. Nishihara, *Handbook of Organic Conductive Molecules and Polymers*, ed. H. S. Nalwa, Wiley, New York, 1997, vol. 2, ch. 19 and refs. therein.
6 R. D. Cannon and R. O. White, *Prog. Inorg. Chem.*, 1988, **36**, 195 and refs. therein.
7 R. Winter, D. T. Pierce, W. E. Geiger and T. J. Lynch, *J. Chem. Soc., Chem. Commun.*, 1994, 1949.
8 T. Weyland, C. Lapinte, G. Frapper, M. J. Calhorda, J.-F. Halet and L. Toupet, *Organometallics*, 1997, **16**, 2024.
9 M. Okuno, K. Aramaki, S. Nakajima, T. Watanabe and H. Nishihara, *Chem. Lett.*, 1995, 585.
10 U. Koelle and F. Khouzami, *Angew. Chem., Int. Ed. Engl.*, 1980, **19**, 640.
11 W. P. Anderson, W. D. Edwards and M. C. Zerner, *Inorg. Chem.*, 1986, **25**, 2728.
12 G. N. Schrauzer, *Acc. Chem. Res.*, 1969, **2**, 72.
13 C. Creutz, *Prog. Inorg. Chem.*, 1983, **30**, 1 and refs. therein.
14 M. Okuno, K. Aramaki and H. Nishihara, *J. Electroanal. Chem. Interfacial Electrochem.*, 1997, **438**, 79.
15 R. W. Callahan, G. M. Brown and T. J. Meyer, *J. Am. Chem. Soc.*, 1974, **96**, 7829; *Inorg. Chem.*, 1975, **14**, 1443.
16 M. D. Todd, Y. Dong and J. T. Hupp, *Inorg. Chem.*, 1991, **30**, 4685.
17 M. J. Powers, R. W. Callahan, D. J. Salmon and T. J. Meyer, *Inorg. Chem.*, 1976, **15**, 894.
18 N. S. Hush, *Prog. Inorg. Chem.*, 1967, **8**, 391.
19 M. B. Robin and P. Day, *Adv. Inorg. Chem. Radiochem.*, 1967, **10**, 247.
20 W. Weitner, jun., *Magnetic Atoms and Molecules*, Dover, New York, 1989, pp. 236–243.

Received 23*rd April* 1998; *Paper* 8/03028F